DNA wrapping is required for DNA damage recognition in the *Escherichia coli* DNA nucleotide excision repair pathway

Hailin Wang[a,b], Meiling Lu[a], Moon-shong Tang[c], Bennett Van Houten[d,1], J. B. Alexander Ross[e], Michael Weinfeld[f,2], and X. Chris Le[a,2]

[a]Department of Laboratory Medicine and Pathology, University of Alberta, Edmonton, AB, Canada T6G 2G3; [b]State Key Laboratory of Environmental Chemistry and Ecotoxicology, Research Center for Eco-Environmental Sciences, Chinese Academy of Sciences, Beijing 100085, China; [c]Department of Environmental Medicine, New York University, Tuxedo, NY 10987; [d]National Institute of Environmental Health Sciences, Research Triangle Park, NC 27709; [e]Department of Chemistry and Biochemistry and BioSpectroscopy Core Research Laboratory, University of Montana, Missoula, MT 59812; and [f]Experimental Oncology, Cross Cancer Institute, Edmonton, AB, Canada T6G 1Z2

Edited by Philip C. Hanawalt, Stanford University, Stanford, CA, and approved May 12, 2009 (received for review March 3, 2009)

Localized DNA melting may provide a general strategy for recognition of the wide array of chemically and structurally diverse DNA lesions repaired by the nucleotide excision repair (NER) pathway. However, it is not clear what causes such DNA melting and how it is driven. Here, we show a DNA wrapping–melting model supported by results from dynamic monitoring of the key DNA–protein and protein–protein interactions involved in the early stages of the *Escherichia coli* NER process. Using an analytical technique involving capillary electrophoresis coupled with laser-induced fluorescence polarization, which combines a mobility shift assay with conformational analysis, we demonstrate that DNA wrapping around UvrB, mediated by UvrA, is an early event in the damage-recognition process during *E. coli* NER. DNA wrapping of UvrB was confirmed by Förster resonance energy transfer and fluorescence lifetime measurements. This wrapping did not occur with readily denaturable damaged DNA substrates ("bubble" DNA), suggesting that DNA wrapping of UvrB plays an important role in the induction of DNA melting around the damage site. Analysis of DNA wrapping of mutant UvrB Y96A further suggests that a cooperative interaction between DNA wrapping of $UvrA_2B$ and contact of the β-hairpin of UvrB with the bulky damage moiety may be involved in the local DNA melting at the damage site.

capillary electrophoresis | laser induced fluorescence polarization | *Bacillus caldotenax* | fluorescence resonance energy transfer

Nucleotide excision repair (NER) displays a unique capability of recognizing and processing a broad spectrum of bulky lesions, which are chemically and structurally diverse (1, 2). In *Escherichia coli*, the complex of UvrA and UvrB is responsible for damage search and recognition along DNA (1, 3). A number of models have been proposed to explain the repair of the broad spectrum of substrates acted on by the *E. coli* NER, including the helicase-scanning model (4–6), the damage-processing model (7), and the padlock model (8, 9). The key difference among these models is the mechanism of damage recognition. In the helicase-scanning model, the $UvrA_2B$ complex locates damage through a helicase-driven translocation step. In the damage-processing model, the $UvrA_2B$ complex finds damage by random diffusion. Accumulating evidence shows that local DNA melting around the damage site induced by the UvrAB complex provides a structural basis for efficient incision of damaged nucleotides by the UvrB and UvrC proteins (10–12). These observations form the basis for the padlock model. Recently, crystal structure analysis of UvrB–DNA complexes has provided evidence that also supports the padlock model (13, 14). However, the mechanism responsible for DNA melting remains to be elucidated. It has been proposed that DNA wrapping around NER proteins may be pertinent to the recognition of the broad spectrum of repairable substrates (15–17). There is a need to confirm this proposition with experiments conducted under dynamic conditions.

In the present study, we have monitored the key DNA–protein and protein–protein interactions involved in the early stages of the *E. coli* NER pathway using a method employing capillary electrophoresis coupled with laser-induced fluorescence polarization (CE-LIFP). The combination of 2 measurements, CE migration time and polarization value, provides information on the formation and properties of biomolecular complexes. The use of this technology enabled us to systematically study the DNA wrapping of UvrB along the course of the *E. coli* NER pathway by constructing well-defined damaged DNA probes. We demonstrate that DNA wrapping of UvrB occurs in several key steps of *E. coli* NER, thereby inducing the local melting of DNA around the damage site and stabilizing the DNA–protein complex.

Results

UvrB Binding to Damaged DNA Induces Large Polarization that Is Independent of Molecular Size. Our initial probe, TMR-BP-ds90mer, comprised a double-stranded oligonucleotide of 90 bp that contained a single (−)-*trans*-anti-benzopyrene diol epoxide (BPDE)-N^2-dG adduct in the middle of one chain and a tetramethylrhodamine (TMR) label at the 5′ end of the same chain (18) (see supporting information (SI) Tables S1 and S2 for description of all oligonucleotide sequences and substrates used in this study). The BPDE adduct functioned as a recognizable DNA lesion for UvrAB proteins, while the TMR served as a suitable label for measurement of fluorescence intensity and polarization. Fig. 1*A* shows the electropherograms obtained from CE-LIFP analysis (19) of TMR-BP-ds90mer and the mixtures of TMR-BP-ds90mer with UvrA or UvrA and UvrB. UvrA can form a homodimer and further bind to TMR-BP-ds90mer to form a heterotrimeric complex, $UvrA_2$•TMR-BP-ds90mer. This complex (migration time 1.68 min) was well separated from the unbound TMR-BP-ds90mer (2.15 min) (Fig. 1*A*, traces 1 and 2). UvrB alone did not form a DNA–protein complex, consistent with previous reports that UvrA is required to load UvrB onto the damage sites (8, 20). In the presence of UvrA and UvrB together, 2 UvrB-containing complexes,

Author contributions: H.W., M.L., M.W., and X.C.L. designed research; H.W., M.L., and X.C.L. performed research; M.-s.T., B.V.H., and J.B.A.R. contributed new reagents/analytic tools; H.W., M.L., M.-s.T., B.V.H., J.B.A.R., M.W., and X.C.L. analyzed data; and H.W., M.L., B.V.H., M.W., and X.C.L. wrote the paper.

The authors declare no conflict of interest.

This article is a PNAS Direct Submission.

Freely available online through the PNAS open access option.

[1]Present address: Hillman Cancer Center, Department of Pharmacology and Chemical Biology, University of Pittsburgh, Pittsburgh, PA 15213.

[2]To whom correspondence may be addressed. E-mail: xc.le@ualberta.ca or michaelw@cancerboard.ab.ca.

This article contains supporting information online at www.pnas.org/cgi/content/full/0902281106/DCSupplemental.

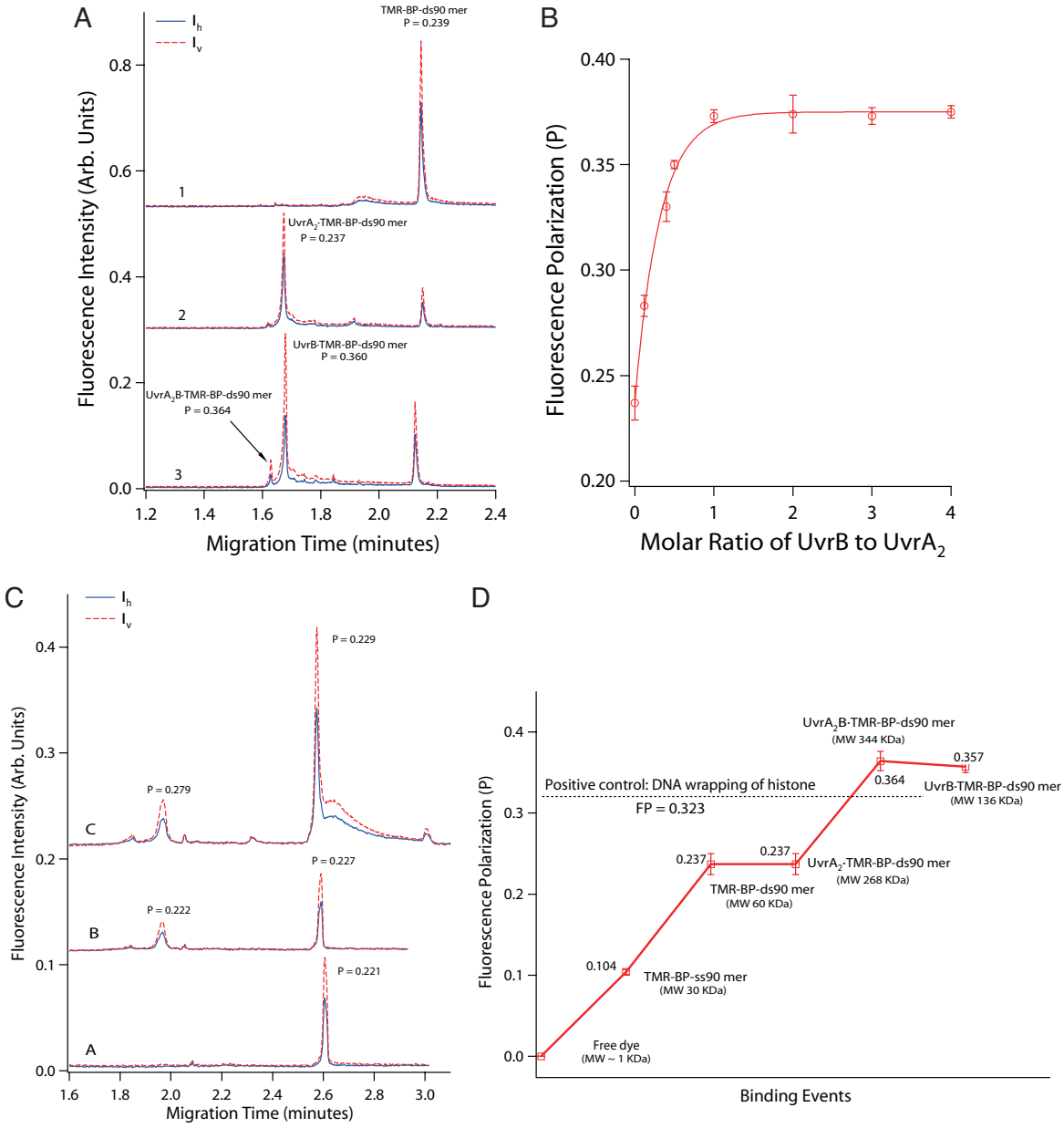

Fig. 1. CE-LIFP analysis of the interaction of fluorescent DNA substrates with *E. coli* UvrA and B proteins. (*A*) CE-LIFP analysis of TMR-BP-ds90mer and its binding to UvrAB, showing a large increase of fluorescence polarization (P). The reaction solutions contained 10 nM TMR-BP-ds90mer (trace 1); 10 nM TMR-BP-ds90mer and 20 nM UvrA (trace 2); or 10 nM TMR-BP-ds90mer, 20 nM UvrA, and 40 nM UvrB (trace 3). The solid and dashed lines represent horizontally (I_h) and vertically (I_v) polarized fluorescence, respectively. (*B*) UvrB concentration-dependent increase of fluorescence polarization of UvrAB-TMR-BP-ds90mer complex. TMR-BP-ds90mer and UvrA were kept at 10 and 20 nM, respectively, and UvrB was varied from 0 to 40 nM. (*C*) CE-LIFP analysis of the mixtures of unmodified TMR-ds90mer with UvrA and UvrB proteins, showing a lack of increase in fluorescence polarization after UvrB binding to undamaged DNA. Shown are 10 nM TMR-ds90mer (trace A), 10 nM TMR-ds90mer + 20 nM UvrA (trace B), and 10 nM TMR-ds90mer + 20 nM UvrA + 40 nM UvrB (trace C). (*D*) Fluorescence-polarization values of DNA–protein intermediates generated along the initial steps of the *E. coli* NER pathway from TMR-BP-ds90mer, UvrA binding to TMR-BP-ds90mer, UvrA and UvrB binding to TMR-BP-ds90mer, and UvrB binding to TMR-BP-ds90mer. Fluorescence-polarization values for free dye (TMR) and TMR-BP-ss90mer were also measured for comparison.

$UvrA_2$UvrB·TMR-BP-ds90mer (1.62 min) and UvrB·TMR-BP-ds90mer (1.68 min), were observed (Fig. 1*A*, trace 3). Although UvrB·TMR-BP-ds90mer had the same migration time as $UvrA_2$·TMR-BP-ds90mer, it had a markedly higher fluorescence-polarization value (P > 0.36). A titration of $UvrA_2$·TMR-BP-ds90mer with UvrB revealed a concentration-dependent increase in fluorescence polarization with increasing UvrB up to a 1:1 molar ratio of UvrB to $UvrA_2$·TMR-BP-ds90mer (Fig. 1*B*). These results indicate that binding of UvrB to the substrate is responsible for the high fluorescence polarization values.

The 2 UvrB–DNA complexes display similar large fluorescence polarization but different CE migration times, probably as a result of their difference in molecular mass (344 kDa vs. 136 kDa) because they have similar negative charge (attributed mainly to the ds90mer). The identities of the 2 observed UvrB–DNA complexes were confirmed through the use of nonhydrolyzable ATPγS (Fig. S1).

To test for nonspecific binding and its fluorescence polarization, we used a probe with the same sequence as TMR-BP-ds90mer but lacking the BPDE lesion. UvrA alone or together with UvrB displayed ≈50-fold lower affinity ($K_a \approx 1.1 \times 10^7$ M^{-1}) for TMR-ds90mer and could not induce a large increase in the P value (P = 0.222 for UvrA–DNA complex; P = 0.279 for UvrB–DNA

complexes) (Fig. 1*C*). In contrast, the binding of $UvrA_2B$ to TMR-BP-ds90mer has a $K_a \approx 6.0 \times 10^8$ M^{-1} and a polarization value of P = 0.36. These results indicate that the large polarization value of UvrB–DNA complexes is associated with damage-specific recognition by UvrB.

The results of fluorescence polarization obtained from Fig. 1*A* are summarized in Fig. 1*D*. The initial increase in fluorescence polarization probably reflects the increase in the molecular size of these fluorescent species, from the free TMR label (≈0.5 kDa, negligible polarization) to TMR-BP-ss90mer (≈30 kDa, P = 0.104), TMR-BP-ds90mer (≈60 kDa, P = 0.237), and the UvrA complex with the TMR-BP-ds90mer (≈267 kDa, P = 0.237). These results are consistent with fluorescence polarization being dependent on molecular size up to ≈40 kDa (when further increase in size does not lead to an increase in fluorescence polarization) (21). Thus, the substantial increase in polarization when UvrA and UvrB are simultaneously bound to the same TMR-BP-ds90mer molecule ($UvrA_2B$·TMR-BP-ds90mer, ≈344 kDa, P = 0.364) cannot be explained by the increase in molecular size alone. Furthermore, the ensuing dissociation of UvrA from the complex of $UvrA_2B$·TMR-BP-ds90mer to generate UvrB·TMR-BP-ds90mer does not significantly decrease polarization (≈136 kDa, P = 0.357).

Large polarization values were also observed upon UvrB binding with other types of damaged DNA, including (+) *trans*-anti-BPDE-ds90mer (i.e., the same oligonucleotide bearing a different BPDE isomer) and internally labeled fluorescein (FAM)-ds90mer (Table S3). The results indicate that the large polarization resulting from UvrB–DNA complexes does not depend on the specific structure of the bulky lesions.

DNA Wrapping of UvrB Is Responsible for the Large Polarization Value of UvrB Complexes. What causes the large polarization response when UvrB binds to TMR-BP-ds90mer (P ≈ 0.36, ΔP ≈ 0.12)? It is evident that it is not dependent on molecular size in comparison with the binding of UvrA to ds90mer, which does not induce significant polarization change (P = 0.237, ΔP ≈ 0). Likewise, the difference in molecular size between UvrB complex and $UvrA_2B$ complex does not produce a corresponding polarization difference (ΔP = −0.007). Previously, it has been shown that $UvrA_2B$ or UvrB binding to the damage may induce DNA wrapping (17, 22). Moreover, it has been consistently shown that DNA does not undergo wrapping when complexed to UvrA in the absence of UvrB, irrespective of whether UvrA is bound to the damage or not (15, 17, 23, 24). By comparing the DNA wrapping behavior and polarization response of UvrB with those of UvrA, we hypothesized that the DNA wrapping of UvrB is responsible for the large polarization response of UvrB–DNA complexes.

This hypothesis was experimentally tested by CE-Förster resonance energy transfer (CE-FRET). The DNA wrapping of UvrB induces a DNA conformational change and should shorten the distance between 2 ends of a DNA probe, which should be discernible by FRET. To conduct this experiment, a FRET-BP-ds90mer that contained a single BPDE-dG adduct in the middle of one chain and was labeled with one FRET donor dye (6-carboxylfluorescein, FAM) and one acceptor dye (TMR) at the 5′ ends of the opposing strands was designed. The measurement of FRET was achieved by exciting labeled FAM at 488 nm and monitoring the fluorescence emissions of FAM at 515 nm and TMR at 580 nm, respectively. The increase of the latter over the background indicates FRET from FAM to TMR, which can be estimated by using the fluorescence ratio measured at 580 nm and 515 nm, an approach that avoids interference from fluorescence quenching unrelated to FRET.

We observed that FRET indeed occurred upon binding of FRET-BP-ds90mer to UvrB. The ratio of fluorescence at Em580 to Em515 nm increased from 0.71 ± 0.05 to 1.16 ± 0.24 and 1.00 ± 0.05 ($n = 3$) for the $UvrA_2B$·FRET-BP-ds90mer and UvrB·FRET-BP-ds90mer, respectively. Taking into account the limited distance over which FRET can occur (10 nm) and the linear distance between the 2 dyes in the unbound FRET-BP-ds90mer (≈29 nm), the observation of significant FRET suggests a dramatic conformational change of FRET-BP-ds90mer after UvrB binding. We attribute this to the DNA wrapping induced by UvrB binding.

UvrA binding to DNA has not been reported to induce DNA wrapping, and there was no FRET observed for the FRET-BP-ds90mer before and after UvrA binding. Their corresponding fluorescence ratios of Em580 nm to Em515 nm were 0.71 ± 0.05 and 0.75 ± 0.08, respectively.

The conformational change of DNA in UvrB–DNA complexes was also confirmed by the time-resolved fluorescence lifetime analysis (see Table S4). The binding of TMR-BP-ds90mer to *E. coli* UvrAB caused an average lifetime increase from 2.044 ns to 2.212 ns. The optimal fitting of the intensity decay data suggests that close contact of the protein(s) to the TMR in the damage probe results in significant restriction of the local rotation of TMR and this restriction of the local rotation of TMR leads to increased polarization of the fluorescence. This result also supports our hypothesis that the large polarization values are linked to DNA wrapping of UvrB.

DNA Wrapping of UvrB Protein Induces Multipoint Contact that May Contribute to the Large Polarization Response. Based on the data described above, we hypothesize that, due to DNA wrapping around UvrB, the TMR attached to the 5′end of the damaged 90-mer comes into close contact with UvrB and the local rotation of the TMR probe is restricted (modeled in Fig. 2*A*); this results in the large polarization response of UvrB–DNA complexes. If this hypothesis is correct, the polarization value for UvrB–DNA complexes should depend on the distance between the damage site and the fluorescent tag. The UvrB complex of a longer damaged probe, in which the TMR tag is beyond the close contact site with UvrB, should not display a large polarization value.

To test this hypothesis, we further investigated the polarization of UvrB–DNA complexes by using 5 damaged DNA probes with lengths of 50 bp, 70 bp, 80 bp, 90 bp, and 105 bp. The measured polarization values are plotted against DNA length in Fig. 2*B*. Short DNA probes (≤70 bp), which are insufficient to wrap around UvrAB (17), displayed a moderate fluorescence polarization response (P = 0.233–0.261), whereas the 2 probes with lengths of 80 bp and 90 bp displayed large polarization responses after UvrAB binding (P = 0.343 ± 0.016 and 0.364 ± 0.012). The large polarization is consistent with the restricted rotational motion of the fluorophore due to proper wrapping of the DNA around the protein. However, the UvrAB complex of the longest DNA probe (105 bp) displayed only a moderate polarization value (P = 0.207 ± 0.15), suggesting that the rotational movement of the end-labeled TMR is not restricted because the wrapping by the longer DNA leaves the TMR dangling free (as shown schematically in Fig. 2*A*).

To confirm that the high polarization value arises from restricted rotation of the fluorophore, TMR-ds90mer was incubated with a preparation of calf thymus histone H1. Histone H1 makes intimate contact with DNA in a sequence-independent manner through both its globular and its lysine-rich carboxy-terminus (25). The complex of the histone with TMR-ds90mer indeed exhibited (see Fig. S2) a large polarization value (P = 0.323). In contrast, the DNA probe TMR-ds90mer alone gave a moderate polarization response (P = 0.176).

DNA Wrapping Is Important for DNA Strand Opening. If wrapping is necessary for opening the DNA, then we hypothesize that if UvrB is presented with DNA that is already melted, the need for wrapping should be alleviated. To test this hypothesis, we analyzed DNA wrapping of UvrB by a DNA substrate bearing a "bubble" structure, TMR-Bubble-45thFAM-ds90mer. In this substrate, the "damage" took the form of a fluorescein-labeled thymidine at base 45 flanked by 2 mismatched bases on the 3′ side and 3 mismatched bases on the 5′ side. The designed bubble size (6 mismatched base pairs) matches the size that is presumed to exist in the preincision complex

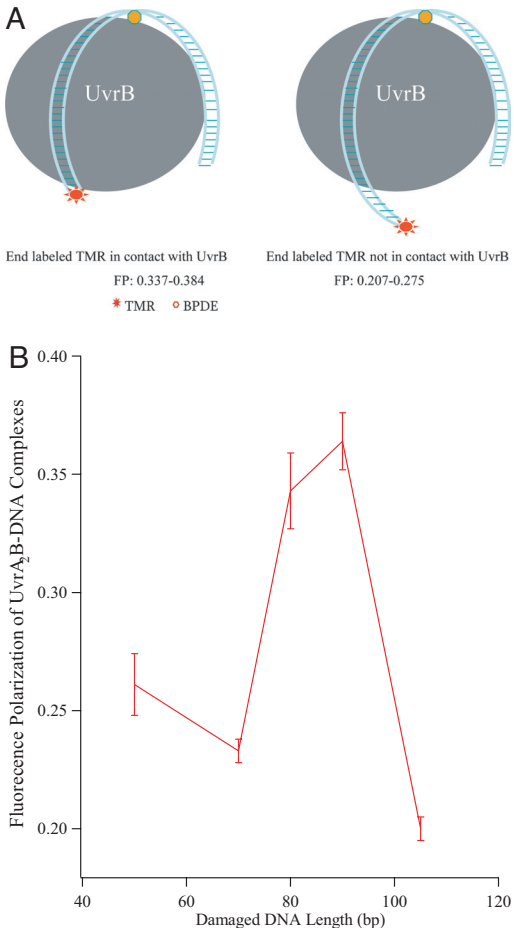

Fig. 2. DNA wrapping of UvrB. (*A*) Schematic illustration of DNA wrapping of UvrB. Long DNA probes can be wrapped by UvrB, leading to multiple sites of contact between DNA and protein. The complexes would display large polarization responses if the end-labeling dye comes into close contact with the protein (*Left*), but only a moderate polarization value if the end-labeling TMR does not contact the protein because the DNA probe is too long (*Right*). Oligonucleotide duplexes that are too short to wrap around UvrB would not be expected to exhibit enhanced fluorescence polarization (not shown). (*B*) The fluorescence polarization of UvrAUvrB–DNA complexes as a function of damaged DNA length, confirming multipoint contact and its role in the large fluorescence-polarization response. The oligonucleotide sequences are shown in Table S2.

(UvrB–DNA) (12). We observed that UvrB binding to the bubble DNA probe only gave a moderate fluorescence-polarization response (P = 0.250 ± 0.016) (see Fig. 3). In contrast, when UvrB was bound to the probe with the same damage (FAM-dT at the 45th base) and using the same end-label (5′-TMR) but without any mismatched base around the damage site, the complex did display a large fluorescence-polarization response (P = 0.349 ± 0.016) (see Fig. 3), which is consistent with the occurrence of DNA wrapping. The lack of DNA wrapping by the bubble DNA suggests that the damaged DNA with preexisting opened strands does not require DNA wrapping to form the preincision complex and further suggests a role played by DNA wrapping of UvrB in strand opening of damaged DNA.

We then asked a fundamental biological question, whether DNA wrapping is important in thermophiles. We hypothesized that DNA wrapping is not necessary for thermophiles because the high temperature of the organisms' habitat is sufficient for localized DNA melting without the need for the facilitation by DNA wrapping. To test this hypothesis, we compared the interaction of damaged probes with UvrA and UvrB proteins originating from

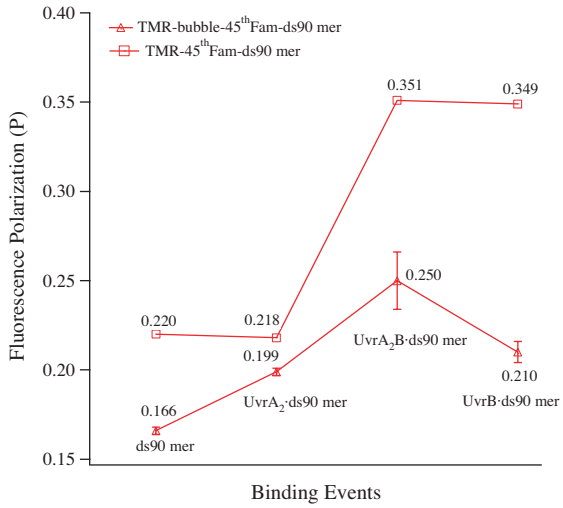

Fig. 3. The course of fluorescence polarization of a bubble DNA substrate vs. binding events, showing no DNA wrapping of the UvrB–bubble DNA complexes. The probe, TMR-bubble-45thFAM-ds90mer, contains 2 mismatched bases on the 3′ side and 3 on the 5′ side to the damaged nucleotide (45th FAM-dT) and is labeled by TMR at the 5′ end of the chain containing 45th FAM-dT. A probe with the same damage (45th FAM-dT), same fluorescence label, and same DNA length but without the bubble was used as control.

E. coli (a mesophile) and *Bacillus caldotenax* (a thermophile). We found that the DNA wrapping of UvrB was coordinated by UvrA from *E. coli* but not from *B. caldotenax* (Fig. 4). Under coordination of *E. coli* UvrA, UvrB from either *B. caldotenax* or *E. coli* formed stable complexes of UvrB-TMR-BP-ds90mer that displayed a large polarization response (P = 0.37–0.38), indicating that damaged DNA wrapped around UvrB. However, UvrB complexes of TMR-BP-ds90mer, coordinated by UvrA from *B. caldotenax*, displayed only a moderate polarization response (P =

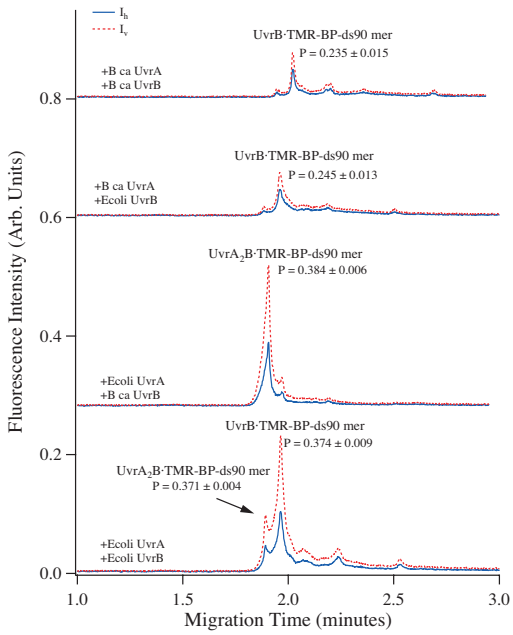

Fig. 4. CE-LIFP analysis of TMR-BP-ds90mer and its binding to *E. coli* UvrAB and *B. caldotenax* UvrAB, showing that the DNA wrapping after UvrB binding to the probe is directed by UvrA. In this experiment, the reaction solutions contained 10 nM TMR-BP-ds90mer, 20 nM UvrA, and 50 nM UvrB. The reactions of UvrA, UvrB, and TMR-BP-ds90mer were conducted at 37 °C.

0.235–0.245), suggesting that the damaged DNA was not wrapped. Time-resolved fluorescence lifetime analysis further indicated the occurrence of significant conformational change after *B. caldotenax* UvrB was loaded by *E. coli* UvrA onto TMR-BPDE-ds90mer (UvrAB-DNA complex $\tau = 2.451$ ns vs. oligo $\tau = 2.044$ ns) and no conformational change when *B. caldotenax* UvrAB bound to the probe TMR-BPDE-ds90mer (UvrAB-DNA $\tau = 2.01$ ns and oligo $\tau = 2.04$ ns) (see Table S4). *B. caldotenax*, a thermophilic bacterium, has an optimal growth temperature of 80 °C (26). UvrA from *B. caldotenax* could not coordinate the DNA wrapping of UvrB on damaged DNA regardless of the incubation temperature tested, 37 °C or 55 °C. We infer that because the temperature of this organism's habitat is so high, DNA melting does not need to be facilitated by its UvrAB wrapping, unlike in *E. coli*.

DNA Wrapping of Mutant UvrB Proteins. We examined the DNA wrapping of mutant *B. caldotenax* UvrB proteins coordinated by *E. coli* UvrA (see Fig. S3). The complexes of UvrAB and TMR-BP-ds90mer formed by all 3 *B. caldotenax* UvrB proteins (wtUvrB, UvrBY96A, and UvrBΔ4) displayed large polarization values (P = 0.329–0.384), indicating that DNA wrapped around these mutant UvrB proteins as well as the wtUvrB protein. Deletion of domain 4 (UvrBΔ4), responsible for dimerization of UvrB (27) and interaction with UvrC, did not affect DNA wrapping of UvrB (P = 0.364), suggesting that domain 4 is not essential for the DNA wrapping of UvrB. However, the binding of TMR-BP-ds90mer to the mutant UvrBY96A gave a lower fluorescence polarization value (P = 0.329) than the binding to wtUvrB (P = 0.384) or to the mutant UvrBΔ4, possibly indicating a lesser degree of DNA wrapping of this mutant UvrB.

In consideration of this mutation, it should be noted that amino acid Tyr-96 in UvrB is 100% conserved among all known UvrB proteins, and it is located at the base of the β-hairpin facing the damaged DNA strand. Mutant UvrBY96A can bind UvrA, can form the UvrAB·DNA complex, and has high DNA-stimulated ATPase, but it exhibits defects in strand-destabilizing activity (28). No stable preincision complex of UvrB·DNA was observed here (Fig. S4), consistent with previous work (28). Because the mutant UvrBY96A has lost its damage-specific recognition ability and strand-destabilizing activity, the observed DNA wrapping of UvrBY96A may suggest that DNA wrapping takes place before damage-specific recognition, indicating that DNA wrapping may be involved in the process of searching for the damage along DNA. However, such DNA wrapping is relatively loose. In comparison, wtUvrB and UvrBΔ4, which possess an efficient strand-destabilizing ability by the β-hairpin, displayed an ability to wrap DNA in a tight manner. The association of tighter DNA wrapping with the efficient strand-destabilizing ability suggests that there is a cooperative interaction between DNA wrapping of UvrB and the strand-destabilizing activity of the β-hairpin, which mutually enhances their activities and leads to the tight DNA wrapping and optimal DNA melting around the damage site.

We also showed that DNA wrapping of UvrB stabilizes the UvrB–DNA complexes (see *SI Text* and Fig. S5 *A* and *B*). The binding constant for the UvrB-gapped DNA complex was >30-fold higher than that for the normal end-labeled DNA.

Discussion

Role of DNA Wrapping in *E. coli* NER. UvrB plays a central role in *E. coli* NER from damage recognition to dual incision, oligonucleotide removal, and repair synthesis, and interacts with all of the components of the system (except DNA ligase), including UvrA, UvrC, UvrD (helicase II), DNA polymerase I, and DNA (2). This study monitors the dynamic process of DNA wrapping of UvrB occurring in several steps of the *E. coli* NER pathway, including UvrAUvrB searching for the damage site (P = 0.364 ± 0.012), dissociation of UvrA and formation of the preincision complex (P = 0.357 ± 0.007), recruitment of UvrC and formation of the incision complex (P = 0.362), and the postincision complexes (P = 0.366 ± 0.007). It is therefore reasonable to conclude that UvrB-induced DNA wrapping plays a key role(s) in *E. coli* NER. Since the first observation of DNA bending, it has been proposed that DNA bending or wrapping may provide a unified mechanism for the NER DNA-damage recognition of a broad spectrum of distinct substrates (15). However, the biological role of DNA wrapping in UvrB recognition of DNA damage is not yet clear. It has been shown, however, that DNA wrapping of UvrB greatly enhances excision efficiency, but it has been assumed that wrapping is not essential to excise DNA lesions because NER can act on short DNA (ds50mer), which cannot wrap UvrB (17). Considering the dependence on DNA length by the strand-destabilizing activity of UvrB and its elimination for longer DNA (>50 bp), currently no persuasive evidence is available to ascertain whether *E. coli* UvrAB can access the damage site in long DNA in the absence of DNA wrapping.

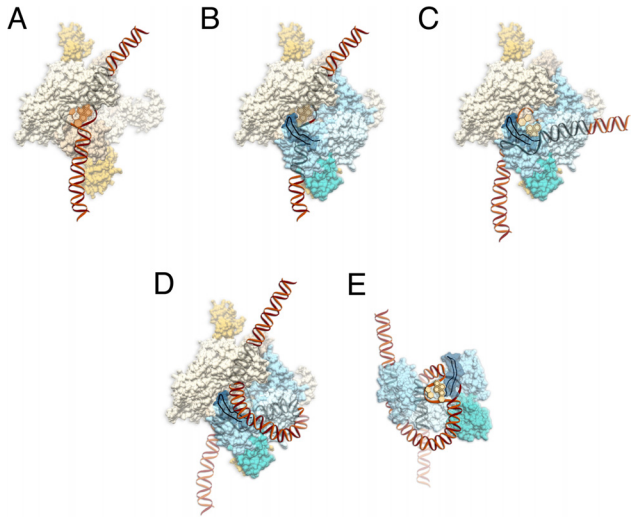

Fig. 5. Hypothetical molecular model of DNA wrapping by UvrA and UvrB. (*A*) UvrA (olive; PDB ID code 2R6F) dimer first interacts with DNA, causing a slight bend. The DNA is expected to make major contact with the region shown in yellow. (*B*) UvrB (light blue; PDB ID code 2FDC) interacts with the domain of UvrA shown in gold, through domain 2 of UvrB (aqua). The β-hairpin is shown in blue, and the ribbon diagram is at the UvrA–DNA–UvrB interface. (*C*) The DNA is transferred from UvrA to the β-hairpin of UvrB, and the DNA becomes highly bent. (*D*) DNA wrapping is facilitated by UvrA around UvrB. (*E*) Full engagement of the DNA by UvrB helps to trigger the release of UvrA, leaving the fully wrapped DNA around UvrB.

In this work, we demonstrate that DNA wrapping of UvrB may enhance DNA melting around the damage site in the damage-recognition process of *E. coli* NER. DNA wrapping was observed in *E. coli* UvrAB recognition of DNA damage, but not observed in its recognition of bubble DNA, suggesting a link between DNA melting (simulated by the DNA bubble) and DNA wrapping of UvrB. In the bubble DNA, no force is required to induce DNA melting and counteract the constant DNA reannealing force because the bubble region around the damage site is produced by 6 mismatched base pairs. Thus, DNA wrapping may provide free energy to counteract reannealing of melted base pairs and thereby enhance and maintain DNA melting during *E. coli* NER. This proposition was also supported by the *B. caldotenax* UvrAB experiments. No wrapping was observed for *B. caldotenax* UvrA or *B. caldotenax* UvrA and UvrB. These data suggest that during repair in thermophilic organisms, the high temperature obviates the need for DNA wrapping to melt the DNA to allow insertion of UvrB's β-hairpin for the formation of a stable preincision complex (13, 29).

DNA Wrapping–Melting Model. Based on current and previous findings, a 2-step DNA wrapping–melting model in *E. coli* NER is

GENETICS

proposed for DNA-damage processing (Fig. 5). For illustration purposes and clarity, we have shown a dimer of UvrA first binding to DNA without UvrB, but the UvrAB complex is mostly likely the actual damage-recognition machine in which lesion detection first occurs through a UvrA interaction and the DNA is partially bent (30) (Fig. 5*A*). The recent crystal structure of a UvrA dimer by Verdine and coworkers (31) and our recent work (32) have suggested a path for DNA across the UvrA dimer. Verdine and coworkers (31) have suggested an independently folding domain of UvrA (shown in gold), which is believed to be important for UvrB interaction, and we have shown this region of UvrA (shown in gold) interacting with domain 2 of UvrB (shown in aqua) (Fig. 5*B*). Recently, Verdine and coworkers have solved the co-crystal structure of a fragment of UvrA and a portion of domain 2 of UvrB that form the binding interface between the two proteins (38). Using atomic force microscopy, we (27) and Goosen and coworkers (22, 33) have suggested that UvrB can form a dimer in solution and on DNA. For clarity, only one monomer of UvrB is shown in Fig. 5, in which the β-hairpin (dark blue) is facing down toward UvrA. UvrA and UvrB working together may amplify or convert the slight helix distortion resulting from the lesions into a denatured state around the damage site. The enhanced short-range melting of DNA around the damage site allows UvrB to insert its β-hairpin between the 2 strands to interact with the bulky damage (Fig. 5*C*). In the next step, DNA wrapping of UvrAB and the strand-destabilizing action of the β-hairpin of UvrB may cooperatively interact with each other, leading to local melting of DNA and stable and tight DNA wrapping around the damage site (Fig. 5*D*). In the final step, UvrA is released and the DNA remains stably wrapped around UvrB (Fig. 5*E*). In the proposed model, DNA wrapping and resultant DNA melting provide a common structural basis for NER recognition of a diverse range of DNA lesions.

Methods

Protein–DNA Interaction. The *E. coli* UvrA, UvrB, and UvrC proteins were produced and purified as previously described (34), and *B. caldotenax* UvrA, wtUvrB, UvrBY96A, and UvrBΔ4 proteins were prepared following published protocols (28, 30, 35). The damage probes and the oligonucleotides for their synthesis are listed in Tables S1 and S2. Binding of the UvrA or UvrA and UvrB was conducted in final reaction solutions containing 50 mM Tris-HCl (pH 7.5), 85 mM KCl, 10 mM $MgCl_2$, 1 mM DTT, 1 mM ATP, 10% glycerol (vol/vol), 5 nM or 10 nM damaged probe, 0–40 nM UvrA, and 0–40 nM UvrB. After 1-h incubation at 37 °C, the solutions were immediately subjected to CE-LIFP analysis.

CE-LIFP. The CE-LIFP analyses were conducted on laboratory-built CE systems with laser-induced fluorescence polarization (LIFP) detectors (19, 36, 37). Fused-silica capillaries (20 μm i.d. × 30 cm, 150 μm o.d.) (Polymicro Technologies) were used for CE separation. Aliquots of the reaction solutions containing UvrAB proteins and DNA probes (in 50 mM Tris-HCl, 85 mM KCl, and 10 mM $MgCl_2$) were electrokinetically injected into the capillary by applying an injection voltage of 20 kV for 5 seconds. Separation was carried out at room temperature with a voltage of 20 kV and a running buffer containing 1.5 × TG [37 mM Tris, 288 mM glycine (pH 8.3)]. The TMR-labeled probes were excited at 543.5 nm, and the fluorescence was detected at 580 nm. The polarization (P) was determined by measuring vertically and horizontally polarized fluorescence (I_v and I_h) and calculated according to the following equation (21):

$$P = \frac{I_v - I_h}{I_v + I_h} \quad [1]$$

Detailed information on the design of DNA damage probes, CE-FRET, time-resolved fluorescence lifetime analysis, and binding constant estimation is shown in *SI Text*.

ACKNOWLEDGMENTS. We thank Dr. Oleg Kovalsky (Johns Hopkins University, Baltimore, MD) for providing reagents, Dr. Xing-Fang Li (University of Alberta) for valuable discussion and suggestions, and Dr. Sue Edelstein (National Institute of Environmental Health Sciences) for preparing Fig. 5. This work was supported by the Canadian Institutes of Health Research, the National Cancer Institute of Canada (X.C.L. and M.W.), the Natural Sciences and Engineering Research Council of Canada, the Canada Research Chairs Program, the Canadian Water Network, Alberta Water Research Institute, and Alberta Health and Wellness (X.C.L.), 973 Project Grant 2008CB417201 (to H.W.), Natural Science Foundation of China Grants 20677066 and 20621703 (to H.W.), National Institutes of Health Grant P20 RR-15583 (to J.B.A.R.), National Science Foundation Grant MCB-0517644 (to J.B.A.R.), and the National Institutes of Health National Institute of Environmental Health Sciences Intramural Program (B.V.H.).

1. Friedberg EC, et al. (2006) DNA repair and mutagenesis (ASM Press, Washington, DC), 2nd Ed, pp 229–239.
2. Truglio JJ, Croteau DL, Van Houten B, Kisker C (2006) Prokaryotic nucleotide excision repair: The UvrABC system. *Chem Rev* 106:233–252.
3. Sancar A, Reardon JT (2004) Nucleotide excision repair in *E. coli* and man. *Adv Protein Chem* 69:43–71.
4. Oh EY, Grossman L (1987) Helicase properties of the *Escherichia coli* UvrAB protein complex. *Proc Natl Acad Sci USA* 84:3638–3642.
5. Oh EY, Grossman L (1989) Characterization of the helicase activity of the *Escherichia coli* UvrAB protein complex. *J Biol Chem* 264:1336–1343.
6. Koo HS, Claassen L, Grossman L, Liu LF (1991) ATP dependent partitioning of the DNA template into supercoiled domains by *Escherichia coli* UvrABC. *Proc Natl Acad Sci USA* 88:1212–1216.
7. Gordienko I, Rupp WD (1997) The limited strand-separating activity of the UvrAB protein complex and its role in the recognition of DNA damage. *EMBO J* 16:889–895.
8. Theis K, Chen PJ, Skorvaga M, Van Houten B, Kisker C (1999) Crystal structure of UvrB, a DNA helicase adapted for nucleotide excision repair. *EMBO J* 18:6899–6907.
9. Theis K, et al. (2000) The nucleotide excision repair protein UvrB, a helicase-like enzyme with a catch. *Mutat Res* 460:277–300.
10. Gordienko I, Rupp WD (1997) UvrAB activity at a damaged DNA site: Is unpaired DNA present? *EMBO J* 16:880–888.
11. Zou Y, Walker R, Bassett H, Geacintov NE, Van Houten B (1997) Formation of DNA repair intermediates and incision by the ATP-dependent UvrB-UvrC endonuclease. *J Biol Chem* 272:4820–4827.
12. Zou Y, Van Houten B (1999) Strand opening by the $UvrA_2B$ complex allows dynamic recognition of DNA damage. *EMBO J* 18:4889–4901.
13. Truglio JJ, et al. (2006) Structural basis for DNA recognition and processing by UvrB. *Nat Struct Mol Biol* 13:360–364.
14. Waters TR, Eryilmaz J, Geddes S, Barrett TE (2006) Damage detection by the UvrABC pathway: Crystal structure of UvrB bound to fluorescein-adducted DNA. *FEBS Lett* 580:6423–6427.
15. Shi Q, Thresher R, Sancar A, Griffith J (1992) Electron microscopic study of (A)BC excinuclease. DNA is sharply bent in the UvrB-DNA complex. *J Mol Biol* 226:425–432.
16. Hsu DS, et al. (1994) Flow linear dichroism and electron microscopic analysis of protein-DNA complexes of a mutant UvrB protein which binds to but cannot kink DNA. *J Mol Biol* 241:645–650.
17. Verhoeven EE, Wyman C, Moolenaar GF, Hoeijmakers JHJ, Goosen N (2001) Architecture of nucleotide excision repair complexes: DNA is wrapped by UvrB before and after damage recognition. *EMBO J* 20:601–611.
18. Carnelley T, et al. (2001) Synthesis, characterization, and applications of a fluorescent probe of DNA damage. *Chem Res Toxicol* 14:1513–1522.
19. Wan Q-H, Le XC (1999) Fluorescence polarization studies of affinity interactions in capillary electrophoresis. *Anal Chem* 71:4183–4189.
20. Orren PK, Sancar A (1989) The (A)BC excinuclease of *Escherichia coli* has only the UvrB and UvrC subunits in the incision complex. *Proc Natl Acad Sci USA* 86:5237–5241.
21. Lakowicz JR (2006) *Principles of Fluorescence Spectroscopy* (Springer, New York), 3rd Ed.
22. Verhoeven EE, Wyman C, Moolenaar GF, Goosen N (2002) The presence of two UvrB subunits in the UvrAB complex ensures damage detection in both DNA strands. *EMBO J* 21:4196–4205.
23. Van Houten B, Gamper H, Sancar A, Hearst JE (1987) DNase I footprint of ABC Excinuclease. *J Biol Chem* 27:13180–13187.
24. Van Houten B, Gamper H, Hearst JE, Sancar A (1988) Analysis of sequential steps of nucleotide excision repair in *Escherichia coli* using synthetic substrates containing single psoralen adducts. *J Biol Chem* 263:16553–16560.
25. Wolffe AP (1997) Histone H1. *Int J Biochem Cell Biol* 29:1463–1466.
26. Heinen UJ, Heinen W (1972) Characteristics and properties of a caldo-active bacterium producing extracellular enzymes and 2 related strains. *Arch Mikrobid* 82:1–23.
27. Wang H, et al. (2006) UvrB domain 4, an autoinhibitory gate for regulation of DNA binding and ATPase activity. *J Biol Chem* 281:15227–15237.
28. Skorvaga M, et al. (2004) Identification of residues within UvrB that are important for efficient DNA binding and damage processing. *J Biol Chem* 279:51574–51580.
29. López-García P (1999) DNA supercoiling and temperature adaptation: A clue to early diversification of life? *J Mol Evol* 49:439–452.
30. DellaVecchia MJ, et al. (2004) Analyzing the handoff of DNA from UvrA to UvrB utilizing DNA-protein photoaffinity labeling. *J Biol Chem* 279:45245–45256.
31. Pakotiprapha D, et al. (2008) Crystal structure of *Bacillus stearothermophilus* UvrA provides insight into ATP-modulated dimerization, UvrB interaction, and DNA binding. *Mol Cell* 29:122–133.
32. Croteau DL, DellaVecchia MJ, Perera L, Van Houten B (2008) Cooperative damage recognition by UvrA and UvrB: Identification of UvrA residues that mediate DNA binding. *DNA Repair* 7:392–404.
33. Moolenaar GF, Schut M, Goosen N (2005) Binding of the UvrB dimer to non-damaged and damaged DNA: Residues Y92 and Y93 influence the stability of both subunits. *DNA Repair* 4:699–713.
34. Nazimiec M, et al. (2001) Sequence-dependent interactions of two forms of UvrC with DNA helix-stabilizing CC-1065-N3-adenine adducts. *Biochemistry* 40:11073–11081.
35. Skorvaga M, Theis K, Mandavilli BS, Kisker C, Van Houten B (2002) The β-hairpin motif of UvrB is essential for DNA binding, damage processing, and UvrC-mediated incisions. *J Biol Chem* 277:1553–1559.
36. Wang H, Lu M, Le XC (2005) DNA-driven focusing for protein-DNA binding assays using capillary electrophoresis. *Anal Chem* 77:4985–4990.
37. Wan Q-H, Le XC (2000) Studies of protein-DNA interactions by capillary electrophoresis laser-induced fluorescence polarization. *Anal Chem* 72:5583–5589.
38. Pakotiprapha D, Liu Y, Verdine GL, Jeruzalmi D (2009) A structural model for the damage-sensing complex in bacterial nucleotide excision repair. *J Biol Chem* 284:12837–12844.